

12

NONLINEAR EFFECTS

The design of a lightwave transmission system requires careful planning and consideration of factors such as fiber selection, choice and tuning of optoelectronic components, optical amplifier placement, and path routing. The goal of this planning is to create a network that meets the design criteria, is reliable, and is easy to operate and maintain. As the previous chapters describe, the design process must take into account all power penalties associated with optical signal-degradation processes.

Intuitively, it seems natural to let the input optical power be as large as possible to overcome the power penalty effects to achieve the link design goals. However, this works only if the fiber is a linear medium; that is, if the loss and refractive index are independent of the optical signal power level. In an actual fiber several different nonlinear effects start to appear as the optical power level increases.¹⁻⁷ These nonlinearities arise when several high-strength optical fields from different signal wavelengths are present in a fiber at the same time and when these fields interact with acoustic waves and molecular vibrations. For example, if the nonlinear threshold for the total launched power into a fiber is 17 dBm (50 mW), then for a 64-channel DWDM link the power limit per wavelength is -1.0 dBm (0.78 mW). Consequences of nonlinear effects for signal levels of this magnitude include power gain or loss at different wavelengths, wavelength conversions, and crosstalk between wavelength channels. In some cases the nonlinear effects can degrade WDM system performance, while in other situations they might provide a useful application.

This chapter first gives a general overview of nonlinear processes in optical fibers in Sec. 12.1. Since the nonlinearities arise above a certain optical power threshold, the effect becomes negligible once the signal has become sufficiently attenuated after traveling a certain distance along the fiber. This gives rise to the concept of an effective length and an associated parameter called effective area, as Sec. 12.2 describes. The next five sections discuss how the major nonlinear processes physically affect system performance. These nonlinearities are *stimulated Raman scattering* (Sec. 12.3), *stimulated Brillouin scattering* (Sec. 12.4), *self-phase modulation* (Sec. 12.5), *cross-phase modulation* (Sec. 12.6), and *four-wave mixing* (Sec. 12.7). Mitigation of four-wave mixing can be achieved by means of a special fiber design or by a *chromatic dispersion-compensation method*, which is the topic of Sec. 12.8. On the other hand, nonlinear effects also can have beneficial uses. Section 12.9 describes applications of cross-phase-modulation and four-wave-mixing techniques for performing wavelength conversion in WDM networks. Another application of nonlinear effects in a silica fiber is the use of solitons for optical communications, which depends on self-phase modulation effects. Section 12.10 addresses this topic.

N2.3 STIMULATED RAMAN SCATTERING

Stimulated Raman scattering is an interaction between lightwaves and the vibrational modes of silica molecules.³⁻⁸ If a photon with energy $h\nu_1$ is incident on a molecule having a vibrational frequency ν_m , the molecule can absorb some energy from the photon. In this interaction, the photon is scattered, thereby attaining a lower frequency ν_2 and a corresponding lower energy $h\nu_2$. The modified photon is called a *Stokes photon*. Because the optical signal wave that is injected into a fiber is the source of the interacting photons, it is often called the *pump wave* because it supplies power for the generated wave.

This process generates scattered light at a wavelength longer than that of the incident light. If another signal is present at this longer wavelength, the SRS light will amplify it and the pump-wavelength signal will decrease in power; Fig. 12.3 illustrates this effect. Consequently, SRS can severely limit the performance of a multichannel optical communication system by transferring energy from short-wavelength channels to neighboring higher-wavelength channels. This is a broadband effect that can occur in both directions.³ Powers in WDM channels separated by up to 16 THz (125 nm) can be coupled through the SRS effect, as Fig. 12.4 illustrates in terms of the Raman gain coefficient g_R as a function of the channel separation $\Delta\nu_s$. This shows that, owing to SRS, the power transferred from a lower-wavelength channel to a higher-wavelength channel increases approximately linearly with channel spacing up to a maximum of about $\Delta\nu_c = 16$ THz (or $\Delta\lambda_c = 125$ nm in the 1550-nm window), and then drops off sharply for larger spacings.

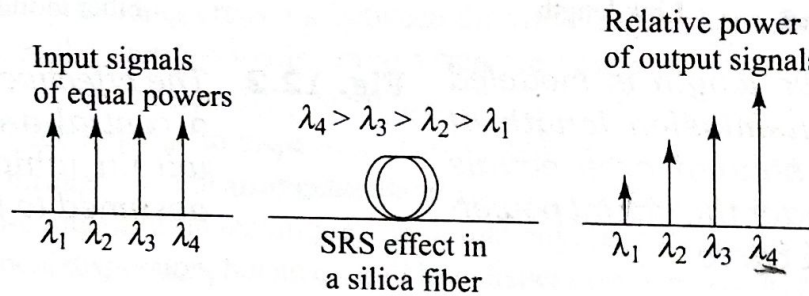


Fig. 12.3 *SRS transfers optical power from shorter wavelengths to longer wavelengths*

To see the effects of SRS, consider a WDM system that has N channels equally spaced in a 30-nm band centered at 1545 nm. Channel 0, which is at the lowest wavelength, is affected the worst because power gets transferred from this channel to all longer-wavelength channels. For simplicity, assume that the transmitted power P is the same on all channels, that the Raman gain increases linearly as shown by the dashed line in Fig. 12.4, and that there is no interaction between the other channels. If $F_{\text{out}}(j)$ is the fraction of power coupled from channel 0 to channel j , then the total fraction of power coupled out of channel 0 to all the other channels is⁹

$$F_{\text{out}} = \sum_{j=1}^{N-1} F_{\text{out}}(j) = \sum_{j=1}^{N-1} g_{R,\text{peak}} \frac{j \Delta\nu_s}{\Delta\nu_c} \frac{PL_{\text{eff}}}{2A_{\text{eff}}} = \frac{g_{R,\text{peak}} \Delta\nu_s PL_{\text{eff}}}{2 \Delta\nu_c A_{\text{eff}}} \frac{N(N-1)}{2} \quad (12.2)$$

The power penalty for this channel then is $-10 \log(1 - F_{\text{out}})$. To keep the penalty below 0.5 dB, we need to have $F_{\text{out}} < 0.1$. Using Eq. 12.2, and with $A_{\text{eff}} = 55 \mu\text{m}^2$ and $g_{R,\text{peak}} = 7 \times 10^{-14} \text{ m/W}$ from Fig. 12.4, gives the criterion

$$[NP][N-1][\Delta\nu_s] L_{\text{eff}} < 5 \times 10^3 \text{ mW} \cdot \text{THz} \cdot \text{km} \quad (12.3)$$

Here, NP is the total power coupled into the fiber, $(N-1)\Delta\nu_s$ is the total occupied optical bandwidth, and L_{eff} is the effective length, which takes into account absorption along the length of the fiber.

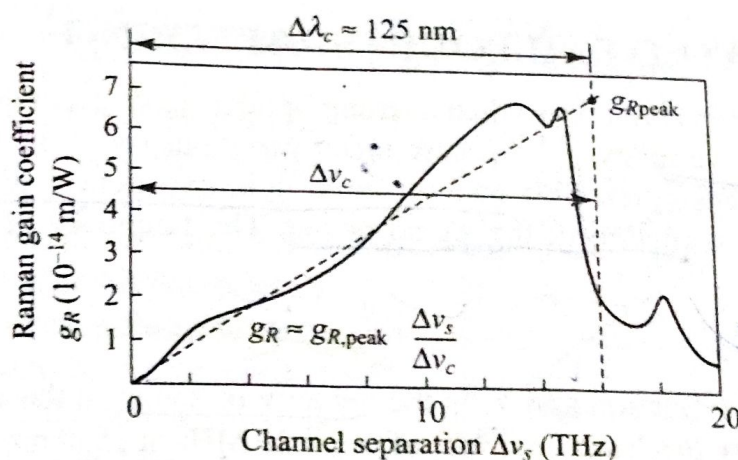


Fig. 12.4 Simplified linear approximation for the Raman gain coefficient as a function of channel spacing. The actual function has some fluctuations about this approximation and a low-value decaying tail of less than $0.5 \times 10^{-8} \mu\text{m/W}$ at channel separations greater than 16 THz

Example 12.1

The limits indicated by Eq. (12.3) are illustrated in Fig. 12.5 for systems with four and eight wavelength channels. The curves show the maximum power per channel as a function of the number of wavelengths for three different channel spacings (recall that a 125-GHz

frequency spacing is equivalent to a 1-nm wavelength spacing at 1550 nm), a fiber attenuation of 0.2 dB/km (or, equivalently, $4.61 \times 10^{-2} \text{ km}^{-1}$), and an amplifier spacing of 75 km (which yields an effective length of $L_{\text{eff}} = 22 \text{ km}$).

The results in Fig. 12.5 were calculated for the worst-case scenario caused by SRS. In general, if the optical power per channel is not excessively high (e.g., less than 1 mW each), then the effects of SRS do not contribute significantly to the eye-closure penalty as a function of transmission distance.^{1.6}

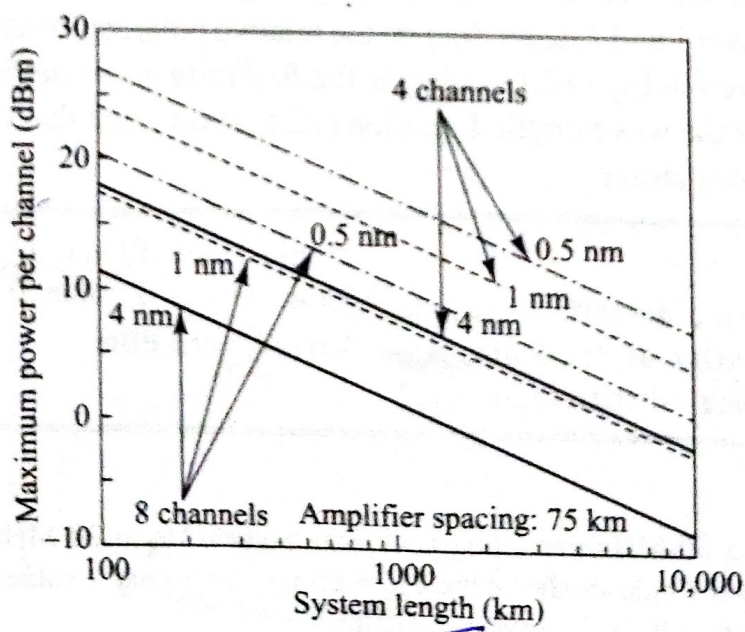


Fig. 12.5 Maximum allowable power per wavelength channel versus transmission length for three different channel spacings. The curves are for the power levels that ensure an SRS degradation of less than 1 dB for all channels. (Reproduced with permission from O'Mahoney, Simeinidou, Yu, and Zhou; J. Lightwave Tech., vol. 13, pp. 817–828, © IEEE, May 1995)

12.4 STIMULATED BRILLOUIN SCATTERING

Stimulated Brillouin scattering arises when a strong optical signal generates an acoustic wave that produces variations in the refractive index.^{1,3,4-10} These index variations cause lightwaves to scatter in the backward direction toward the transmitter. This backscattered light experiences gain from the forward-propagating signals, which leads to depletion of the signal power. The frequency of the scattered light experiences a Doppler shift given by

$$v_B = 2nV_s/\lambda \quad (12.4)$$

where n is the index of refraction and V_s is the velocity of sound in the material. In silica, this interaction occurs over a very narrow *Brillouin linewidth* of $\Delta v_B = 20 \text{ MHz}$ at 1550 nm. For $V_s = 5760 \text{ m/s}$ in fused silica, the frequency of the backward-propagating light at 1550 nm is downshifted by 11 GHz (0.09 nm) from the original signal. This shows that the SBS effect is confined within a *single wavelength channel* in a WDM system. Thus, the effects of SBS accumulate individually for each channel, and, consequently, occur at the same power level in each WDM channel, analogous to a *single-channel system*.

System impairment starts when the amplitude of the scattered wave is comparable to the signal power. For typical fibers, the threshold power for this process is around 10 mW for single-fiber spans. In a long fiber chain containing optical amplifiers, there are normally optical isolators to prevent backscattered signals from entering the amplifier. Consequently, the impairment due to SBS is limited to the degradation occurring in a single amplifier-to-amplifier span.

One criterion for determining at what point SBS becomes a problem is to consider the *SBS threshold power* P_{th} . This is defined to be the signal power at which the backscattered light equals the fiber-input power. The calculation of this expression is rather complicated, but an approximation is given by⁴

$$P_{\text{th}} \approx 21 \frac{(A_{\text{eff}})b}{g_B L_{\text{eff}}} \left(1 + \frac{\Delta v_{\text{source}}}{\Delta v_B} \right) \quad (12.5)$$

Here, A_{eff} is the effective cross-sectional area of the propagating wave, Δv_{source} is the source linewidth, and the polarization factor b lies between 1 and 2 depending on the relative polarizations of the pump and Stokes waves. The effective length L_{eff} is given in Eq. (12.1) and g_B is the *Brillouin gain coefficient*, which is approximately $4 \times 10^{-11} \text{ m/W}$, independent of the wavelength. Equation (12.5) shows that the SBS threshold power increases as the source linewidth becomes larger.

Example 12.2

Consider an optical source with a 40-MHz linewidth. Using the values $\Delta v_B = 20 \text{ MHz}$ at 1550 nm, $A_{\text{eff}} = 55 \times 10^{-12} \text{ m}^2$ (for a typical dispersion-shifted

single-mode fiber), $L_{\text{eff}} = 20 \text{ km}$, and assuming a value of $b = 2$, then from Eq. (12.5) we have $P_{\text{th}} = 8.6 \text{ mW} = 9.3 \text{ dBm}$.

Drill Problem 12.2

Consider an optical source with a 60-MHz linewidth. Using the values $\Delta v_B = 20 \text{ MHz}$ at 1550 nm, $A_{\text{eff}} = 55 \times 10^{-12} \text{ m}^2$ (for a typical dispersion-shifted single-mode fiber), $L_{\text{eff}} = 20 \text{ km}$, assuming a value of $b = 1$, and letting $g_B = 3.5 \times 10^{-11} \text{ m/W}$, show from Eq. (12.5) that $P_{\text{th}} = 5.0 \text{ mW} = 7.0 \text{ dBm}$.

Figure 12.6 illustrates the effect of SBS on unmodulated signal power once the threshold is reached. The plots give the relative Brillouin scattered power and the signal power transmitted through a fiber as a function of the input power. Below a certain signal level called the *SBS threshold*, the transmitted power increases linearly with the input level. The effect of SBS is negligible for these low power levels but becomes greater as the optical power level increases.

Trans. SBS

At the SBS threshold, the SBS process becomes nonlinear and the launched signal loses an increasingly greater percentage of its power as the signal strength becomes larger. Beyond the SBS threshold, the percentage increase in signal depletion continues to grow with signal strength until the SBS limit is reached. Any additional optical power launched into the fiber after this point merely is scattered backward along the fiber due to the SBS effect. Thus above the SBS limit the transmitted power remains constant for higher inputs, since all the added power is extracted from the signal to feed the scattered wave.

In standard G.652 single-mode fiber, the SBS limit restricts the maximum launched optical power to be 17 dBm. As an example of efforts to mitigate this limit, Corning Incorporated designed a G.652-compatible fiber with a 3-dB higher SBS threshold. This new design enables twice as much power (an additional 3 dB) to be launched into the fiber.

Figure 12.7 illustrates the SBS-induced impairment on the carrier-to-noise ratio (CNR) of an amplitude-modulated vestigial-sideband (AM-VSB) video signal for the same fiber as in Fig. 12.6. Here, the CNR grows with increasing fiber-injected power up to the SBS threshold. Beyond this point the CNR starts to decrease.¹¹

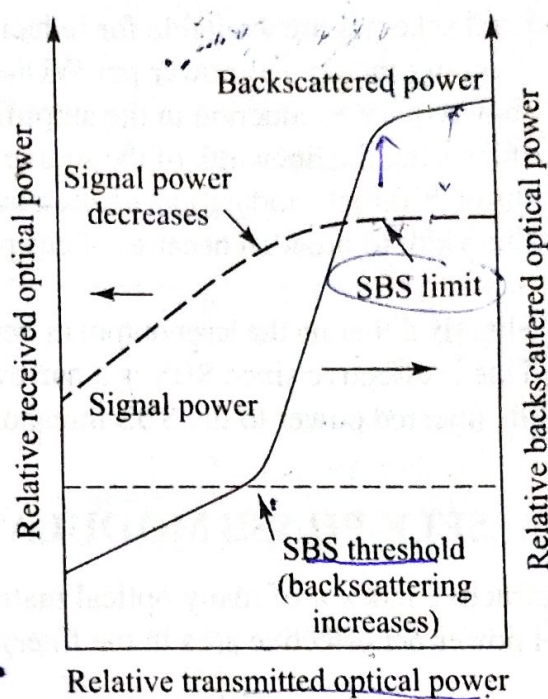


Fig. 12.6 The effect of SBS on signal power in an optical fiber

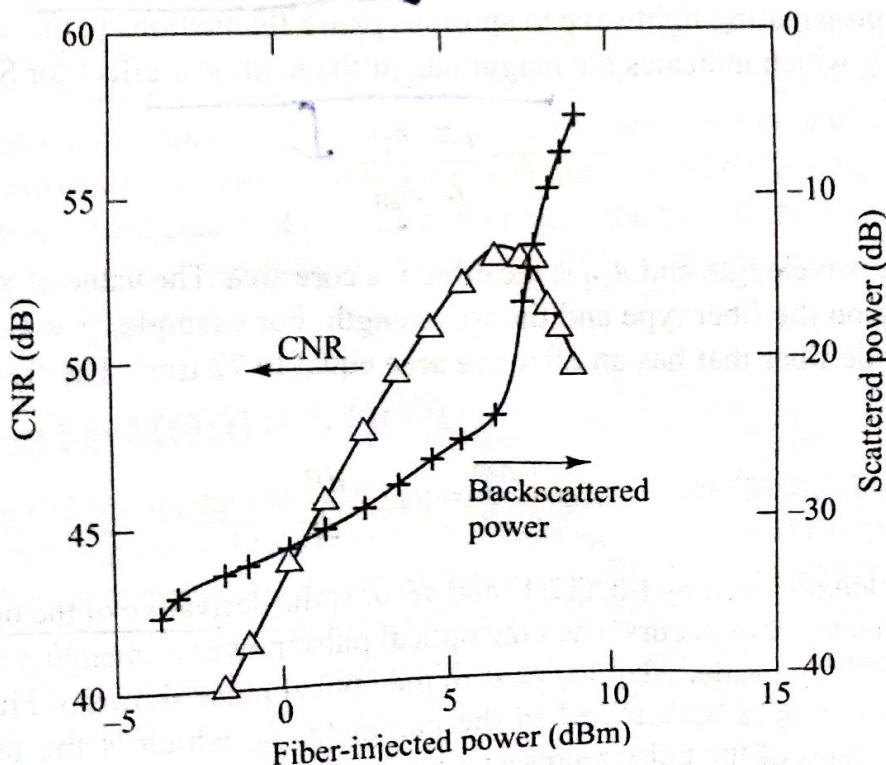


Fig. 12.7 The SBS impairment on the CNR of an AM-VSB signal. The triangles are the CNR and the crosses represent the backscattered power. (Adapted with permission from Mao, Bodeep, Tkach, Chraplyvy, Darcie, and Dorosier,¹¹ © IEEE, 1992)

- Several schemes are available for reducing the power-penalty effects of SBS. These include^{1,3,4,8}
 - Keeping the optical power per WDM channel below the SBS thresholds. For long-haul systems, this may require a reduction in the amplifier spacing.
 - Increasing the linewidth of the source as the gain bandwidth of SBS is very small. This can be achieved through direct modulation of the source (as opposed to external modulation), since this causes the linewidth to broaden because of chirping effects. However, a large dispersion penalty may result from this.
 - Slightly dithering the laser output in frequency, at roughly 100 to 200 MHz to raise the Brillouin threshold. This is effective since SBS is a narrowband process. The dither frequency should scale as the ratio of the injected power to the SBS threshold.

12.5 SELF-PHASE MODULATION

The refractive index n of many optical materials has a weak dependence on *optical intensity* I (equal to the optical power per effective area in the fiber) given by.

$$n = n_0 + n_2 I = n_0 + n_2 \frac{P}{A_{\text{eff}}} \quad (12.6)$$

where n_0 is the *ordinary refractive index* of the material and n_2 is the *nonlinear index coefficient*. The factor n_2 is about $2.6 \times 10^{-8} \mu\text{m}^2/\text{W}$ in silica, between 1.2 and $5.1 \times 10^{-6} \mu\text{m}^2/\text{W}$ in tellurite glasses, and $2.4 \times 10^{-5} \mu\text{m}^2/\text{W}$ in $\text{As}_{40}\text{Se}_{60}$ chalcogenide glass. The nonlinearity in the refractive index is known as the *Kerr nonlinearity*.¹² This nonlinearity produces a carrier-induced phase modulation of the propagating signal, which is called the *Kerr effect*. In single-wavelength links, this gives rise to self-phase modulation (SPM), which converts optical power fluctuations in a propagating lightwave to spurious phase fluctuations in the same wave.^{3-5,13}

The main parameter γ , which indicates the magnitude of the nonlinear effect for SPM, is given by

$$\gamma = \frac{2\pi}{\lambda} \frac{n_2}{A_{\text{eff}}} \quad (12.7)$$

where λ is the free-space wavelength and A_{eff} is the effective core area. The value of γ ranges from 1 to $5 \text{ W}^{-1} \text{ km}^{-1}$ in silica depending on the fiber type and the wavelength. For example, $\gamma = 1.3 \text{ W}^{-1} \text{ km}^{-1}$ at 1550 nm for a standard single-mode fiber that has an effective area equal to $72 \mu\text{m}^2$. The frequency shift $\Delta\phi$ arising from SPM is given by

$$\Delta\phi = \frac{d\phi}{dt} = \gamma L_{\text{eff}} \frac{dP}{dt} \quad (12.8)$$

Here L_{eff} is the effective length given by Eq. (12.1) and dP/dt is the derivative of the optical pulse power; that is, it shows that the frequency shift occurs when the optical pulse power is changing in time.

To see the effect of SPM, consider what happens to the optical pulse shown in Fig. 12.8 as it propagates in a fiber. Here the time axis is normalized to the parameter t_0 , which is the pulse half-width at the $1/e$ -intensity point. The edges of the pulse represent a time-varying intensity, which rises rapidly from zero to a maximum value, and then returns to zero. In a medium having an intensity-dependent refractive index, a time-varying signal intensity will produce a time-varying refractive index. Thus the index at the peak of the pulse will be slightly different than the value in the wings of the pulse. The leading edge will see a positive dn/dt , whereas the trailing edge will see a negative dn/dt .

This temporally varying index change results in a temporally varying phase change, shown by $d\phi/dt$ in Fig. 12.8. The consequence is that the instantaneous optical frequency differs from its initial value ν_0 across the pulse. That is, since the phase fluctuations are intensity-dependent, different parts of the pulse undergo different phase shifts. This leads to what is known as **frequency chirping**, in that the rising edge of the pulse experiences a red shift in frequency (toward lower frequencies or longer wavelengths), whereas the trailing edge of the pulse experiences a blue shift in frequency (toward higher frequencies or shorter wavelengths). Since the degree of chirping depends on the transmitted power, SPM effects are more pronounced for higher-intensity pulses.

For some types of fibers, the time-varying phase may result in a power penalty owing to a GVD-induced spectral broadening of the pulse as it travels along the fiber. In the normal dispersion region the chromatic dispersion is negative [that is, from Eq. (3.25) we have $\beta_2 > 0$] and the group delay decreases with wavelength. This means that since red light has a longer wavelength than blue, the red light travels faster in silica because $n_{\text{red}} < n_{\text{blue}}$ (see Fig. 3.12). Therefore, in the normal dispersion region the red-shifted leading edge of the pulse travels faster and thus moves away from the center of the pulse. At the same time the blue-shifted trailing edge travels slower, and thus also moves away from the center of the pulse. In this case chirping worsens the effects of GVD-induced pulse broadening. On the other hand, in the anomalous dispersion region where chromatic dispersion is positive so that the group delay increases with wavelength, the red-shifted leading edge of the pulse travels slower and thus moves toward the center of the pulse. Similarly, the blue-shifted trailing edge travels faster, and also moves toward the center of the pulse. In this case, SPM causes the pulse to narrow, thereby partly compensating for chromatic dispersion.

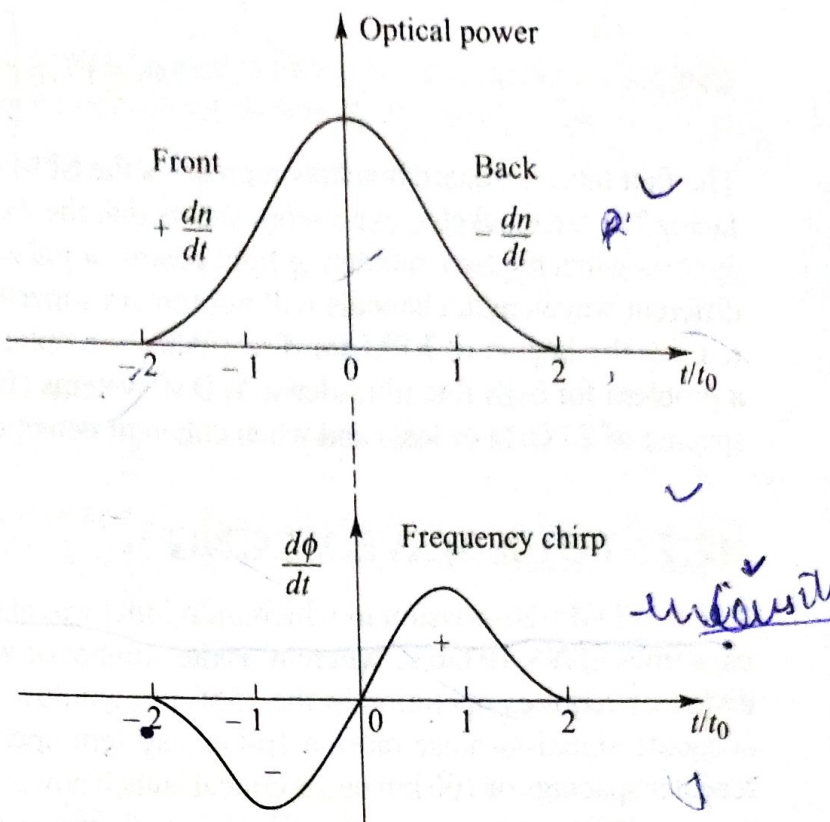


Fig. 12.8 Phenomenological description of spectral broadening of a pulse due to self-phase modulation

12.6 CROSS-PHASE MODULATION

Cross-phase modulation (XPM) appears in WDM systems and has a similar origin as SPM. In this case the name derives from the fact that the refractive index nonlinearity converts optical intensity fluctuations in a particular wavelength channel to phase fluctuations in another copropagating channel.¹⁻⁴ In addition, since the refractive index seen by a particular wavelength is influenced by both the optical intensity of that wave itself and also by the optical power fluctuations of neighboring wavelengths, SPM is always present when XPM occurs. Analogous to SPM, for two interacting wavelengths the XPM-induced frequency shift $\Delta\phi$ is given by

$$\Delta\phi = \frac{d\phi}{dt} = 2\gamma L_{\text{eff}} \frac{dP}{dt} \quad (12.9)$$

where the parameters are the same as for Eq. (12.8). When multiple wavelengths propagate in a fiber, the total phase shift for an optical signal with frequency ω_i is

$$\Delta\phi_i = \gamma L_{\text{eff}} \left[\frac{dP_i}{dt} + 2 \sum_{j \neq i} \frac{dP_j}{dt} \right] \quad (12.10)$$

The first term in square brackets represents the SPM contribution and the second term arises from XPM. The factor 2 in the bracketed expression shows that the weight of XPM is twice that of SPM. However, XPM only appears when the two interacting light beams or pulses overlap in space and time. In general, pulses from two different wavelength channels will not remain superimposed because each has a different GVD. This greatly reduces the impact of XPM for direct-detection optical fiber transmission systems. However, XPM could be a problem for high-rate ultra-dense WDM systems (for example, 2.5- or 10-Gb/s systems with a wavelength spacing of 25 GHz or less) and when coherent detection schemes are used.^{2,3}

12.7 FOUR-WAVE MIXING

Dense WDM transmission in which individual wavelength channels are modulated at rates of 10 Gb/s often capacities of $N \times 10$ Gb/s, where N is the number of wavelengths. To transmit such high capacities over long distances requires operation in the 1550-nm window of dispersion-shifted fiber. In addition, to preserve an adequate signal-to-noise ratio, a 10-Gb/s system operating over long distances and having nominal optical repeater spacings of 100 km needs optical launch powers of around 1 mW per channel. For such WDM systems, the simultaneous requirements of high launch power and low dispersion give rise to the generation of new frequencies due to four-wave mixing.^{1-4,14-16}

Four-wave mixing (FWM) is a third-order nonlinearity in optical fibers that is analogous to intermodulation distortion in electrical systems. When wavelength channels are located near the zero-dispersion point, three optical frequencies (v_i, v_j, v_k) will mix to produce a fourth intermodulation product v_{ijk} given by

$$v_{ijk} = v_i + v_j - v_k \quad \text{with } i, j \neq k \quad (12.11)$$

When this new frequency falls in the transmission window of the original frequencies, it can cause severe crosstalk.

Figure 12.9 shows a simple example for two waves at frequencies v_1 and v_2 . As these waves copropagate along a fiber, they mix and generate sidebands at $2v_1 - v_2$ and $2v_2 - v_1$. Similarly, three copropagating waves will create nine new optical sideband waves at frequencies given by Eq. (12.11). These sidebands will travel along with the original waves and will grow at the expense of signal-strength depletion. In general, for N wavelengths launched into a fiber, the number of generated mixing products M is

$$M = \frac{N^2}{2}(N-1) \quad (12.12)$$

If the channels are equally spaced, a number of the new waves will have the same frequencies as the injected signals. Thus the resultant crosstalk interference plus the depletion of the original signal waves can severely degrade multichannel system performance unless steps are taken to diminish it.

The efficiency of four-wave mixing depends on fiber dispersion and the channel spacings. Since the dispersion varies with wavelength, the signal waves and the generated waves have different group velocities. This destroys the phase matching of the interacting waves and lowers the efficiency at which power is transferred to newly generated frequencies. The higher the group velocity mismatches and the wider the channel spacings, the lower the four-wave mixing.

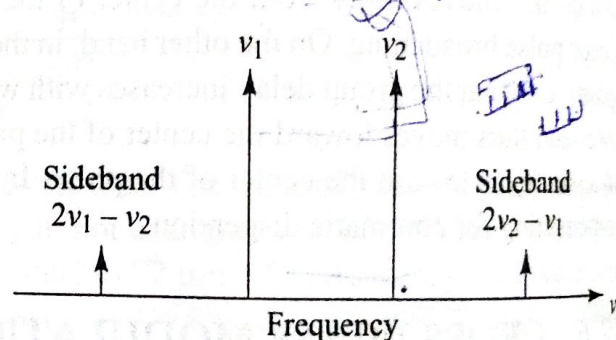


Fig. 12.9 Two optical waves at frequencies v_1 and v_2 mix to generate two third-order sidebands

At the exit of a fiber of length L and attenuation α , the power P_{ijk} that is generated at frequency v_{ijk} due to the interaction of signals at frequencies v_i , v_j , and v_k that have fiber-input powers P_i , P_j , and P_k , respectively, is

$$P_{ijk}(L) = \eta (\mathcal{P})^2 P_i(0) P_j(0) P_k(0) \exp(-\alpha L) \quad (12.13)$$

where the nonlinear interaction constant κ is

$$\kappa = \frac{32\pi^3 \chi_{1111}}{n_2 \lambda c} \left(\frac{L_{\text{eff}}}{A_{\text{eff}}} \right) \quad (12.14)$$

Here, χ_{1111} is the third-order nonlinear susceptibility; η is the efficiency of the four-wave mixing; n is the fiber refractive index; and \mathcal{P} is the degeneracy factor, which has the value of 3 or 6 for two waves mixing or three waves mixing, respectively. The effective length L_{eff} is given by Eq. (12.1) and A_{eff} is the effective cross-sectional area of the fiber. Figure 12.10 gives examples of η as a function of channel spacing for three equally spaced frequencies for dispersion values of a conventional G.652 single-mode fiber [16 ps/(nm · km) average in the 1550-nm window] and a dispersion-shifted G.653 fiber [1 ps/(nm · km) average in the 1550-nm window]. These curves show the frequency-spacing range over which the FWM process is efficient for these two dispersion values (see Prob. 12.5 for a detailed expression for η , which leads to an oscillatory behavior of P_{ijk} as a function of channel spacing). For example, in the conventional single-mode fiber, only frequencies with separations less than 20 GHz will mix efficiently. In contrast, the FWM mixing efficiencies are greater than 20 percent for channel separations up to 50 GHz for G.653 dispersion-shifted fibers.

Example 12.3

Consider a 75-km link of dispersion-shifted single-mode fiber carrying two wavelengths at 1540.0 and 1540.5 nm. The new frequencies generated due to FWM are at

$$\begin{aligned} v_{112} &= 2v_1 - v_2 = 2(1540.0 \text{ nm}) - 1540.5 \text{ nm} \\ &= 1539.5 \text{ nm} \end{aligned}$$

and

$$\begin{aligned} v_{221} &= 2v_2 - v_1 = 2(1540.5 \text{ nm}) - 1540.0 \text{ nm} \\ &= 1541.0 \text{ nm} \end{aligned}$$

Assume the fiber has an attenuation of $\alpha = 0.20 \text{ dB/km} = 0.0461 \text{ km}^{-1}$, a refractive index of 1.48, and a 9.0- μm core diameter, so that $L_{\text{eff}} = 22 \text{ km}$ and $A_{\text{eff}} = 6.4 \times 10^{-11} \text{ m}^2$. From

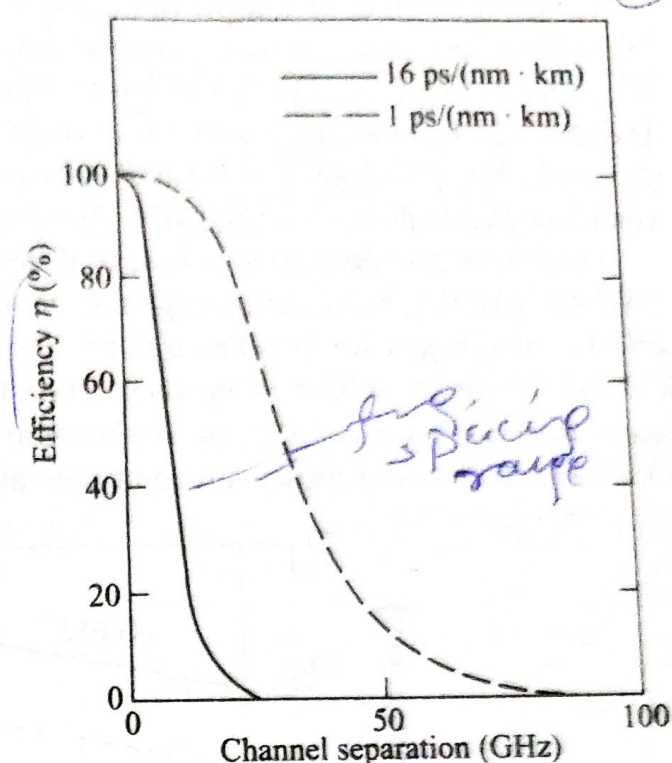


Fig. 12.10 Efficiencies of four-wave mixing as a function of wavelength channel spacing. The solid curve is for standard single-mode fiber with 16 ps/(nm · km) dispersion. The dashed curve is for dispersion-shifted fiber with 1-ps/(nm · km) dispersion. (Reproduced with permission from Chraplyvy, © IEEE, 1990)

Fig. 12.10 we find $\eta \approx 5$ percent for a 62-GHz (0.5-nm) channel spacing. If each channel has an input power of 1 mW, then, using the values $\chi_{1111} = 6 \times 10^{-16} \text{ cm}^3/\text{erg} = 6 \times 10^{-15} \text{ m}^3/(\text{W} \cdot \text{s})$ and $\mathcal{P} = 3$, we find

$$\begin{aligned} P_{112} &= 0.05(3)^2 \left[\frac{32\pi^3 6 \times 10^{-15} \frac{\text{m}^3}{\text{W} \cdot \text{s}}}{(1.48)^2 (1.54 \times 10^{-6} \text{ m}) 3 \times 10^8 \text{ m/s}} \right]^2 \\ &\times \left(\frac{22 \times 10^3 \text{ m}}{6.4 \times 10^{-11} \text{ m}^2} \right)^2 (1.0 \times 10^{-3} \text{ W})^3 \\ &\times \exp[-(0.0461/\text{km})75 \text{ km}] \\ &= 5.80 \times 10^{-8} \text{ mW} \end{aligned}$$